A Kinetic Monte Carlo Method for the Atomic-scale Simulation of Chemical Vapor Deposition: Application to Diamond

ARTICLE *in* JOURNAL OF APPLIED PHYSICS · DECEMBER 1997

Impact Factor: 2.18 · DOI: 10.1063/1.366532 · Source: OAI

3 AUTHORS, INCLUDING:

D.J. Srolovitz
University of Pennsylvania
513 PUBLICATIONS **15,463** CITATIONS

A kinetic Monte Carlo method for the atomic-scale simulation of chemical vapor deposition: Application to diamond

C. C. Battaile and D. J. Srolovitz[a)]
Department of Materials Science and Engineering, University of Michigan, Ann Arbor, Michigan 48109

J. E. Butler
Gas/Surface Dynamics Section, Code 6174, Naval Research Laboratory, Washington, D.C. 20375

(Received 27 December 1996; accepted for publication 15 September 1997)

We present a method for simulating the chemical vapor deposition (CVD) of thin films. The model is based upon a three-dimensional representation of film growth on the atomic scale that incorporates the effects of surface atomic structure and morphology. Film growth is simulated on lattice. The temporal evolution of the film during growth is examined on the atomic scale by a Monte Carlo technique parameterized by the rates of the important surface chemical reactions. The approach is similar to the N-fold way in that one reaction occurs at each simulation step, and the time increment between reaction events is variable. As an example of the application of the simulation technique, the growth of {111}-oriented diamond films was simulated for fifteen substrate temperatures ranging from 800 to 1500 K. Film growth rates and incorporated vacancy and H atom concentrations were computed at each temperature. Under typical CVD conditions, the simulated growth rates vary from about 0.1 to 0.8 μm/hr between 800 and 1500 K and the activation energy for growth on the {111}: H surface between 800 and 1100 K is 11.3 kcal/mol. The simulations predict that the concentrations of incorporated point defects are low at substrate temperatures below 1300 K, but become significant above this temperature. If the ratio between growth rate and point defect concentration is used as a measure of growth efficiency, ideal substrate temperatures for the growth of {111}-oriented diamond films are in the vicinity of 1100 to 1200 K. © *1997 American Institute of Physics.* [S0021-8979(97)05324-3]

INTRODUCTION

Chemical vapor deposition (CVD) is used extensively to produce protective coatings and thin films for electronic devices and optical components. In particular, the growth of diamond films by CVD has received considerable attention lately because of diamond's superlative properties. Diamond is the hardest known material, is resistant to most corrosive substances, has the highest room temperature thermal conductivity, is transparent to optical and infrared radiation, is a wide band gap semiconductor, and has a negative electron affinity.[1–3] Therefore, diamond is ideal for wear- and corrosion-resistant coatings; heat sinks; windows and optical filters; electronic components; and cold cathodes for use in imaging and display applications. However, wide-scale commercial use of high-quality diamond films is limited by high cost and inefficient growth. This is due in part to the complexity and cost of diamond CVD equipment, the slow growth rates (around 1–50 μm/hr)[3] typical of most CVD techniques, and impurities and imperfections incorporated during growth.[4]

Diamond films are typically grown from a precursor gas containing a small amount of hydrocarbon (usually CH_4) in H_2.[2,4,5] This mixture is heated (by a hot filament, microwaves, or DC arc jet), dissociating some of the H_2 into atomic H and creating many different hydrocarbon species.[6–8] Growth is accomplished at subatmospheric pressures (1–200 Torr) where graphite is the stable form of carbon. Atomic H helps stabilize the diamond phase by terminating the diamond lattice with C–H bonds (i.e., passivating the surface), converting sp^2-bonded C into sp^3-bonded diamond, and etching sp^2-bonded C from the surface.[4,5] Growth usually occurs by incorporation of chemisorbed hydrocarbon radicals. Beyond this, our understanding of the atomic mechanisms by which diamond grows remains uncertain.

Since these atomic growth processes are difficult to observe *in situ*, much of our understanding is extracted from modeling and simulation or inferred from experimental observations. While calculations of the energetics of surface states[9–12] can provide the kinetics of individual reaction events, and predictions of surface atomic[13–16] and electronic[17–19] structures are useful in determining the stability of surface atomic configurations, these techniques are inapplicable to the time and length scales required to study diamond film *growth*. One-dimensional growth models[20–23] have been useful for verifying proposed growth mechanisms. However, these models typically consider the kinetics of only one diamond growth mechanism, and do not explicitly account for competing mechanisms or the effects of surface atomic structure and morphology on growth behavior. This is a fundamental shortcoming since the growth of diamond depends strongly on surface atomic configurations and on the coordination of chemisorbed hydrocarbon molecules. The study of these effects requires the simulation of diamond growth on the atomic scale and in three dimensions. Kaukonen and Nieminen[24] have simulated the deposition of diamondlike carbon films using molecular dynamics calculations, but they have not addressed the CVD growth of diamond. Three-dimensional atomic-scale simulations of dia-

a)Electronic mail: srol@umich.edu

mond growth have been performed recently by Dawnkaski *et al.*,[25] but are limited to growth at particular surface configurations on the {100} diamond surface. Diamond growth has also been simulated on the atomic scale by Clark *et al.*,[26] but these studies are limited to milliseconds of growth time.

In this paper we introduce a three-dimensional simulation method for modeling film growth by CVD on virtually any surface. This method incorporates the effects of surface chemistry, atomic structure, and morphology. Although it is applicable to a wide variety of chemical vapor deposition and etching systems, we will focus on the growth of diamond films. The method treats growth on a rigid three-dimensional lattice and is easily capable of simulating *hours* of growth (on common workstations) under most conditions.[27]

The temporal evolution of the film is accomplished by a kinetic Monte Carlo method which is parameterized by conventional surface reaction rate data. The Monte Carlo algorithm is similar to the N-fold way,[28,29] in which a variable time increment is employed to incorporate reaction events that occur on widely different time scales.[30] Because this model treats diamond growth on the atomic scale, it is ideally suited to studying defect generation during growth, and can be used to investigate proposed atomic-scale growth mechanisms. As an example, results from a series of simulations of the growth of {111}-oriented diamond films are presented, the incorporation of defects into {111} films during growth at several substrate temperatures is discussed, and the implications of these results for the optimization of diamond film growth are addressed.

METHOD

The growth of films by CVD occurs by the evolution and incorporation of chemisorbed species on a surface. Diamond is commonly grown in an atmosphere containing H, H_2, and various hydrocarbons. (N, O, and other species are often present as well, and can significantly affect growth behavior,[5,20,31–33] but are not considered here.) Under typical growth conditions, the diamond surface is largely covered by a passivating layer of H atoms.[34–36] Surface sites can be activated by either H desorption or abstraction. Once a diamond surface site is active, it can be repassivated by either a H atom or a hydrocarbon molecule. A chemisorbed hydrocarbon might desorb, returning to the gas phase and reactivating the surface site, or it might be incorporated into the film by subsequent surface reactions leading to film growth. In order to simulate film growth on the atomic scale, the temporal evolution of the occupancy of surface sites must be explicitly represented.

To accomplish this, a lattice with the desired crystallographic orientation is generated and periodic boundary conditions are imposed in the plane perpendicular to the direction of growth. The lattice is rigid, and thus atomic relaxations and vibrations are not explicitly considered (with the exception of dimer bond formation; see below). Diamond growth begins on a smooth H-passivated diamond substrate, which is created by filling the first few atomic layers of the lattice with C atoms and terminating the resulting diamond surface with H atoms. This starting substrate is allowed to interact with a gas containing H, H_2, CH_3, and C_2H_2 according to a predefined set of surface chemical reactions. The rates associated with these reactions are taken from conventional surface reaction kinetics.[21,37,38]

In many applications of the Monte Carlo method, such as the equilibration of atomic positions in a defected crystal, the space of possible configurations that the system can assume is continuous. Therefore, there exists (in principle) an infinite number of new configurations available to the system at any Monte Carlo step. However, since we are simulating CVD growth on a surface of *finite* size which evolves according to a *finite* set of chemical reactions, the number of new configurations available at any Monte Carlo step is *finite* and *enumerable*. This configuration space is discrete. In other words, at each Monte Carlo step, we can determine all of the changes that the system can possibly undergo. Therefore, instead of attempting a random change to the system at each simulation step and then accepting or rejecting that change based on some criterion (e.g., the Metropolis Monte Carlo method[39]), we choose and execute one change from the list of all possible changes at each simulation step. The choice is made based on the relative rates at which each change can occur (i.e., the probability of choosing one particular reaction instead of another is proportional to the rate at which the reaction occurs relative to the rates of the other reactions).

Thus the temporal evolution of the reactive surface molecular species is accomplished by a kinetic Monte Carlo procedure in which one reaction is executed at one site during each time step. Since the starting diamond substrate is completely covered by H atoms, only two *types* of reactions are possible at the first time step: H desorption and H abstraction. Any of the N H atoms that cover the starting substrate can undergo either of these two reactions such that there are $2N$ ''events'' that can occur on the initial surface. That is, either of two reactions (i.e., H desorption or abstraction) can occur at any one of the N reactive sites (i.e., the chemisorbed H atoms). Thus, in the first simulation step, one of these $2N$ possible events is chosen based on the rate associated with that event. More specifically, the probability of choosing an event is equal to the rate at which the event occurs relative to the sum of the rates of all of the possible events. Once an event is chosen, the system is altered appropriately and the set of events that can occur at the *next* time step is updated. So at each time step, one event denoted by m is randomly chosen from all of the M events that can possibly occur at that step, as follows:

$$\frac{\sum_{i=0}^{m-1} r_i}{\sum_{i=0}^{M} r_i} < \xi_1 < \frac{\sum_{i=0}^{m} r_i}{\sum_{i=0}^{M} r_i}, \tag{1}$$

where r_i is the rate at which event i occurs ($r_0 = 0$) and ξ_1 is a random number uniformly distributed in the range (0,1). The way in which the M events are labeled (i.e., by specifying which events correspond to $i = 1,2,3,...,m,\ldots,M$) is arbitrary. After an event is chosen and executed, the total number of possible events, M, and the sequence in which the events are labeled, will change.

A schematic example of this procedure is shown in Fig. 1, which contains the first steps in the evolution of a cluster of diamond surface atoms initially covered by three H atoms.

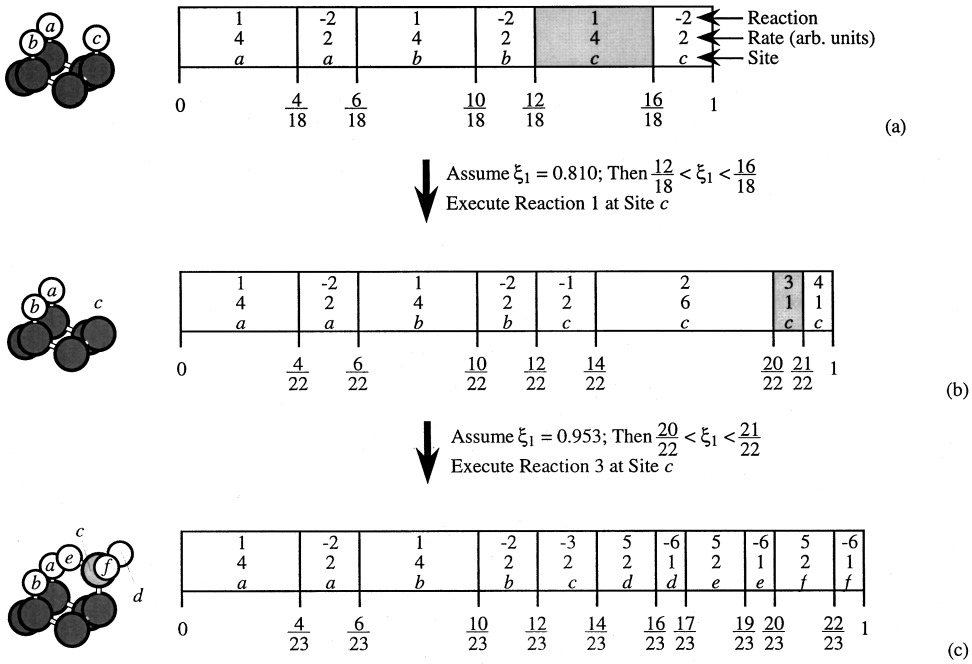

FIG. 1. Example of the first steps in the evolution of a simulated diamond cluster. The simulation starts with (a) a small H-passivated diamond substrate, which undergoes (b) H abstraction and (c) CH_3 chemisorption at site c. Images of the surface are shown at left, and schematics of the lists of running sums of relative reaction rates are shown at right. Dark gray circles are diamond, light gray circles are C atoms in chemisorbed hydrocarbons, and white circles are H atoms. The rates for each reaction are taken from Table I.

For the purposes of this example, we will assume that the system in Fig. 1 can evolve according to the set of reactions and fictitious rates in Table I, where C_d represents a surface diamond atom. Since H is the only reactive species in Fig. 1(a), there are only two *types* of reactions that can occur at the first simulation step: H abstraction by reaction 1 and H desorption by the reverse of reaction 2 (denoted reaction -2). Since there are three surface sites in the diamond cluster, there are six events that can occur at the first simulation step: desorption or abstraction of any one of the three H atoms at sites a, b, and c. To choose one of these six events, a list is constructed which contains a running sum of the rates of each of these six possible events, and each entry in the list is normalized by the sum of the rates of all six events, as shown in Fig. 1(a). The blocks in the list that correspond to H abstraction are twice as long as the blocks corresponding to H desorption, since the rate of H abstraction is twice the rate of H desorption according to the fictitious reaction rates in Table I. Once this list is constructed, a random number, ξ_1, in the range (0,1) is chosen and compared with the numbers in the list of summed relative rates, and one of the six events is chosen according to Eq. (1). If, for example, the random number is chosen to be $\xi_1 = 0.810$, as shown in Fig. 1(a), then the H atom at site c is removed by abstraction. This modifies the system such that the surface is now covered by two H atoms and one surface radical, as shown in Fig. 1(b). According to Table I, a surface radical can react by chemisorption of H (either by reaction 2 or by the reverse of reaction 1), CH_3 (by reaction 3), or C_2H_2 (by reaction 4). Therefore, at the second simulation step, any one of eight events is possible: desorption or abstraction of either of the two H atoms at sites a and b; and chemisorption of H (by one of two mechanisms), CH_3, or C_2H_2 at the surface radical at site c. The list of relative rates is updated to reflect the new configuration, as shown in Fig. 1(b), and one event is again chosen at random, as before. If, for example, chemisorption of CH_3 onto the surface radical is chosen and executed, then *four* new reactive species (one chemisorbed C atom and three H atoms) must be introduced, as shown in Fig. 1(c). The algorithm is repeated as before, and the configuration of adsorbed species evolves accordingly.

TABLE I. Fictitious reaction rates for the example in Fig. 1.

	Reaction	Forward rate (arbitrary units)	Reverse rate (arbitrary units)
1	$C_dH + H \leftrightarrow C_d + H_2$	4	2
2	$C_d + H \leftrightarrow C_dH$	6	2
3	$C_d + CH_3 \leftrightarrow C_dCH_3$	1	2
4	$C_d + C_2H_2 \leftrightarrow C_dC_2H_2$	1	4
5	$C_dCH_3 + H \leftrightarrow C_dCH_2 + H_2$	2	1
6	$C_dCH_2 + H \leftrightarrow C_dCH_3$	3	1

This kinetic Monte Carlo algorithm is similar to the N-fold way method.[28,29] Since one event occurs at each simulation step and different events occur at different rates, the time increment, dt, associated with each simulation step is dynamic and stochastic

$$dt = -\frac{\ln(\xi_2)}{\sum_{i=1}^{M} r_i}, \tag{2}$$

where ξ_2 is a random number uniformly distributed in the range (0,1), and the denominator is the sum of the rates of all of the events that can occur at the simulation step for which

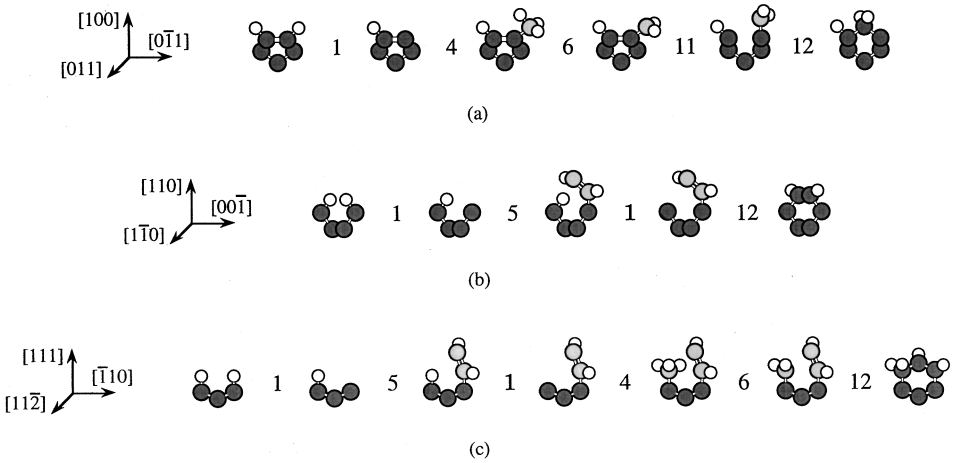

FIG. 2. Examples of reaction sequences leading to growth on the (a) {100}(2×1), (b) {110}, and (c) {111} faces of diamond. The images are schematics of the atomic processes involved in each reaction, and the text between them indicates the reactions, according to the labeling in Table II, that occur between each configuration. Dark gray circles are diamond, light gray circles are C atoms in chemisorbed hydrocarbons, and white circles are H atoms. Dimer bonds are thick white lines, and all other bonds are thin white lines.

dt is being evaluated. The expression for dt in Eq. (2) is rigorous,[28] and a derivation is provided in Appendix A. The N-fold way approach has been shown[29] to be completely interchangeable with (i.e., statistically equivalent to) conventional Monte Carlo schemes that employ a fixed time step. The use of a variable time increment allows the consideration of reactions that occur on widely disparate time scales.[26,30] Whenever very fast reactions are possible, the denominator in Eq. (2) is large and the time increment is small (i.e., the time scale is fine). Conversely, when only slow reactions are possible, the time increment is large (i.e., the time scale is coarse). Thus the time scale automatically and dynamically adjusts to accommodate the fastest possible events at each simulation step, such that the restrictions imposed by the time scale in conventional molecular dynamics and Monte Carlo schemes that use a fixed time increment[25] are greatly reduced.[28,29] A similar approach was recently employed by Clark *et al.*[26] to study the initial stages of growth on the diamond {111} surface. However, these authors combined a kinetic Monte Carlo scheme, like the one described above, with off-lattice atomic relaxations so that their method, while capable of treating the evolution of the diamond surface in considerable detail, is limited to several milliseconds of growth time.[26] Furthermore, previous atomic-scale simulations of diamond CVD growth[25,26] employed a time filter to remove fast processes (e.g., H surface reactions) from the kinetic Monte Carlo calculations, whereas we perform no such filtration.

The preceding discussion describes the algorithm by which the configuration of adsorbed species evolves with time. However, in order to simulate diamond *growth*, a mechanism by which chemisorbed hydrocarbon molecules are converted to diamond must be included. Whenever a hydrocarbon molecule with enough radical sites has two or more C–C bonds to the atoms in the diamond film, all of the C atoms in the hydrocarbon are converted (i.e., relabeled) to diamond C atoms. Examples of the events that can lead to the growth of diamond from CH_3 and C_2H_2 on flat {100}(2×1):H, {110}:H, and {111}:H surfaces are shown in Fig. 2. In each case, growth occurs by completion of the six-atom C ring that is characteristic of the diamond cubic structure. In Fig. 2(a), growth on a dimer reconstructed {100}(2×1):H surface (see below) is initiated by H abstraction from a dimer pair. A CH_3 radical chemisorbs onto the dimer pair, loses one of its H atoms by abstraction, and breaks the dimer bond by a β-scission reaction.[10] It then rotates into the biradical surface site[10] that was left by the broken dimer bond. Growth on a {110}:H surface in Fig. 2(b) starts with H abstraction and C_2H_2 chemisorption onto the diamond surface. After the adjacent H atom is removed from the diamond surface, the upper C atom in the C_2H_2 molecule can bond with the radical on the film. Subsequent growth on the step edges that are created by this growth event can occur by the addition of a single C atom.[4] On the {111}:H surface in Fig. 2(c), growth begins by H abstraction and C_2H_2 chemisorption. H abstraction and CH_3 chemisorption at an adjacent site allow the C_2H_2 molecule to bond to the radical site that is created by H abstraction from the chemisorbed CH_3, thereby forming a three-C diamond bridge. (This three-C bridge easily isomerizes, which can lead to twinning of the lattice,[1] but we shall ignore this phenomenon for the present.) Subsequent growth at this three-C bridge can occur by the addition of one or two C atoms, depending on the growth site. Although this treatment of diamond formation is simplified, it captures most of the kinetic and atomic features that are thought to be important to diamond growth.

Although we consider only the growth of {111} films in this study, the {111} surfaces are free to develop arbitrary morphologies during growth, including {100} microfacets. Therefore, we include in our growth model an explicit atomic-scale treatment of dimer bonding on {100} surfaces. Any biradical on the surface is allowed to dimer bond. In terms of the rigid lattice model used here, whenever two diamond atoms on the surface share an unoccupied site (recall that this model uses a rigid diamond cubic lattice for *all* atomic sites), the two surface atoms can form a dimer bond between them. Any surface diamond atom that is bonded to more than two C atoms (including diamond and hydrocarbon

TABLE II. Reaction rate coefficients for diamond growth (Refs. 21, 37, and 38). A is in units of mol, cm^3, and s; E and ΔH are in units of kcal/mol; and ΔS is in units of cal/(mol·K).

	Reaction	A	n	E	ΔH	ΔS
1	$C_dH+H\leftrightarrow C_d+H_2$	1.3×10^{14}	0	7.3	−9.9	5.3
2	$C_d+H\leftrightarrow C_dH$	1.0×10^{13}	0	0.0	−96.9	−32.8
3	$C_dCH_2+H\leftrightarrow C_d+CH_3$	3.0×10^{13}	0	0.0	−24.6	7.9
4	$C_d+CH_3\leftrightarrow C_dCH_3$	5.0×10^{12}	0	0.0	−70.9	−42.0
5	$C_d+C_2H_2\leftrightarrow C_dC_2H_2$	8.0×10^{10}	0	7.7	−19.0	−10.7
6	$C_dCH_y+H\leftrightarrow C_dCH_{y-1}+H_2$	2.8×10^{7}	2	7.7	−11.3	6.6
7	$C_dCH_y+H\leftrightarrow C_dCH_{y+1}$	1.0×10^{13}	0	0.0	−83.0	−34.1
8	$C_dC_2H_y+H\leftrightarrow C_dC_2H_{y-1}+H_2$	9.0×10^{6}	2	5.0	−8.9	8.7
9	$C_dC_2H_y+H\leftrightarrow C_dC_2H_{y+1}$	2.0×10^{13}	0	0.0	−47.7	−36.2
10	$C_dCH_y+CH_3\rightarrow C_dC_2H_{y+3}$	5.0×10^{12}	0	0.0	⋯	⋯
11	$C_d-C_d\leftrightarrow C_d+*+C_d$	1.0×10^{13}	0	0.0	4.9	0.4
12	$C_d+*+C_dC_xH_y\rightarrow C_d+C_dC_{x-1}H_y+C_d$	2.0×10^{13}	0	8.8	⋯	⋯

chemisorbates) cannot form a dimer bond, and a dimer bond can only open (break) if one or both of the dimer bonded surface atoms is adjacent to a radical hydrocarbon. This latter condition represents dimer opening by β-scission, as suggested by Garrison *et al.*[10] and discussed in detail elsewhere.[21,25] Growth on dimer reconstructed facets can occur by β-scission and ''dimer insertion'',[10,21,25] as shown in Fig. 2(a) and discussed above, or by the bonding of a radical hydrocarbon species into the surface ''trough'' created by two adjacent non-dimer-bonded surface diamond atoms.[25,40] This treatment of dimer bonding allows for the reconstruction and growth of {100} facets in accordance with experiments[41,42] and presently accepted theory,[10,14,16,18] and permits arbitrary dimer patterns and dimer domain structures.

The model of diamond growth presented here is based upon several assumptions that deserve mention. First, the rigid lattice approximation prevents consideration of atomic relaxations. However, since diamond bonds are very rigid, and because we are focusing on growth rather than detailed atomic relaxation, this limitation is not important. Second, although typical CVD diamond growth temperatures are high (around 1200 K, they are low compared to the Debye temperature of diamond (approximately 1900 K) and, hence, atomic vibrations are neglected. Third, since the growth temperature is low compared to covalent bond strengths, the mobility of adsorbates on the surface is neglected. Fourth, since reaction rate coefficients corresponding to all possible chemical reactions at all possible surface sites do not exist, we assume that the reaction rates are unaffected by slight variations in local environment. For example, hydrogen desorption from the {110} face occurs at the same rate as from the {111} face. Although this approach is not ideal, and could easily be remedied if the appropriate reaction rate data were available (e.g., from a series of *ab initio* molecular dynamics calculations), we do not expect this to be severe in light of the large differences between the rates of different reactions and the effects of atomic coordination on growth.[27] Fifth, we have not included the formation of extended defects during growth, and in particular we do not consider twinning of the lattice which is particularly important on the {111} surface of diamond. Defects are known to affect crystal growth behavior, and enhanced growth at reentrant corners on twinned surfaces is probably of particular importance in diamond CVD. Hence the specific results quoted here serve only to illustrate the utility of this technique and should not be compared directly with growth results for which twinning or other extended defects are important. The extension of this method to twinned lattices is straightforward but cumbersome. In addition, the treatment of atomic relaxations and vibrations in a rigid lattice model such as this is not trivial, but the inclusion of surface diffusion and the effects of stereochemistry on surface reaction kinetics relies only on the availability of the relevant data.

RESULTS AND DISCUSSION

As an example of how this model can be used to predict growth behavior, we consider the growth of {111}-oriented diamond films. The conditions at the surface of the growing diamond film represent typical environments in hot-filament and microwave-plasma CVD reactors.[7,8,20,23,25,43–46] Evolution of the reactive surface species occurs according to the chemical reactions in Table II.[21,38,40] C_d represents a surface diamond atom. Species separated by a dash (-) are dimer bonded, and an asterisk (*) represents a surface biradical. Forward rate constants are $k_f=AT^n\exp(-E/RT)$ and reverse rate constants are $k_r=CAT^n\exp(-\Delta S/R)\exp[(\Delta H-E)/RT]$, where C is a constant that accounts for the fact that ΔH and ΔS correspond to a standard state of 1200 K and 1 atm, and is equal to 1.016×10^{-5} mol·cm^{-3}/atm for reactions where the number of moles changes (i.e., the number of products and reactants are unequal) and unity otherwise. Reaction 11 represents dimer bonding of surface atoms, and reaction 12 represents insertion of a hydrocarbon into an opened dimer bond. The growth of {111}-oriented films was simulated at fifteen substrate temperatures between 800 and 1500 K. The starting configuration for each simulation is a flat {111}-oriented diamond substrate containing 300 *surface* C atoms passivated by H atoms. Data were extracted from simulations in which approximately 60 atomic layers (18 000 atoms) were grown, requiring a few hours of computer time per simulation on a desktop workstation. The defect concentrations at each temperature were obtained by averaging the results from four films representing the growth of approximately 72 000 total atoms at each temperature.

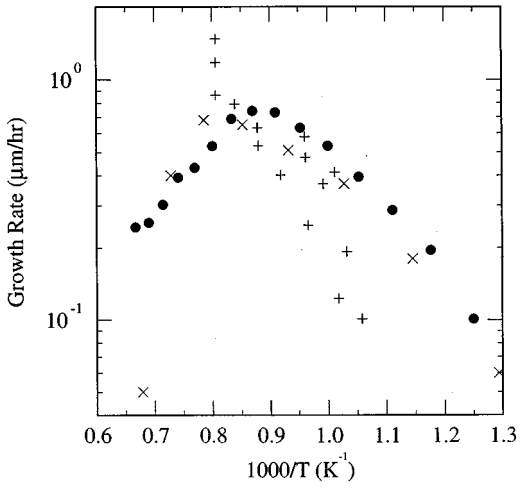

FIG. 3. Growth rates of {111} films for various substrate temperatures in an environment containing 0.04, 18, 0.004, and 0.04 Torr partial pressure of H, H_2, CH_3, and C_2H_2, respectively. Growth rate data from the present simulations (filled circles), from the measurements of Chu *et al.* (Ref. 47) (+), and from the one-dimensional simulations of Frenklach and Wang (Ref. 20) (×) are shown.

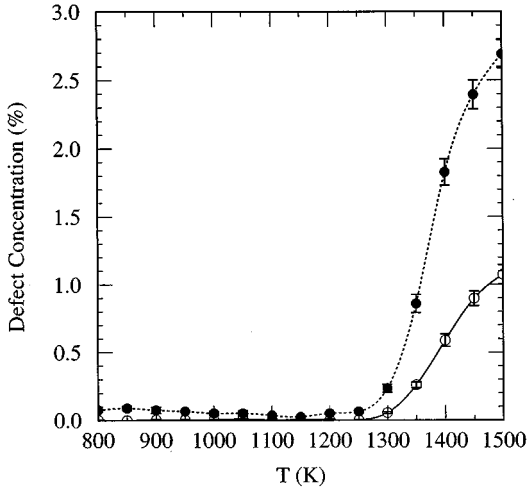

FIG. 4. Concentrations of vacancies (open circles) and H atoms (filled circles) in {111} films as a function of substrate temperature in an environment containing 0.04, 18, 0.004, and 0.1 Torr partial pressure of H, H_2, CH_3, and C_2H_2, respectively. Error bars represent standard deviations over four simulations at each temperature.

Growth rates as a function of substrate temperature are shown in Fig. 3 for an environment containing 0.04, 18, 0.004, and 0.04 Torr partial pressure of H, H_2, CH_3, and C_2H_2, respectively. Values of approximately 0.1 to 0.8 μm/hr between 800 and 1500 K agree well with the experiments of Chu *et al.*[47] and the one-dimensional simulations of Frenklach and Wang,[20] which are plotted in Fig. 3 for comparison. The calculated activation energy for growth between 800 and 1100 K is approximately 11.3 kcal/mol, in good agreement with values of 12.0 kcal/mol between 1000 and 1250 K measured by Chu *et al.*[47] and 10.8 kcal/mol between 773 and 1173 K predicted by Frenklach and Wang.[20] The rate of CH_3 incorporation is much higher than C_2H_2 incorporation (see Table II), and growth rates decrease with temperature at high temperatures in Fig. 3 because the rate of CH_3 desorption (reaction -4) becomes high. Since incorporation of C atoms at step edges is preferred over incorporation on terrace sites,[27] the film morphologies consist of multiple layers of flat terrace bounded by jagged atomic-height steps.

Defects are incorporated during growth whenever a vacant or H atom site is completely covered by the growth of diamond material around and over that site. Since we do not require that diamond grow at every lattice site, it is possible for nondiamond sites to become encased by diamond material, and thereby isolated from the growth atmosphere, as growth progresses around and above the nondiamond site. When this occurs in the course of a simulation, the encased site is prohibited from participating in further reactions and is thereby trapped in the film as a point defect. The concentrations of incorporated vacancies and H atoms are plotted in Fig. 4 as a function of substrate temperature for an environment containing 0.04, 18, 0.004, and 0.1 Torr partial pressure of H, H_2, CH_3, and C_2H_2, respectively. The majority of the incorporated point defects are H atoms since the diamond surface is mostly covered by H atoms at the temperatures studied. The point defect concentrations are low at substrate temperatures below 1300 K, but become substantial above this temperature. This behavior is due to the relative contributions to growth from CH_3 and C_2H_2. A CH_3 radical can chemisorb into nearly covered sites on the growing surface that C_2H_2 cannot fit into. A nearly enclosed site might be filled by a CH_3 radical but merely covered by C_2H_2. Therefore, C_2H_2 can more effectively trap point defects than can CH_3. Even though relatively little growth occurs from C_2H_2, the incorporation of point defects increases as C_2H_2 becomes more important (relative to CH_3) to the growth process. As mentioned above, the desorption of CH_3 becomes very rapid at high temperatures. This leads to a decrease in the growth rates at high temperatures, since the growth rates depend largely on the contribution to growth from CH_3. However, since defect incorporation depends on the competition between C_2H_2 and CH_3 growth, a decrease in growth from CH_3 effectively increases the relative contribution to growth from C_2H_2, thereby increasing the concentrations of point defects.[48]

The efficient production of high-quality diamond films requires that growth rates are maximized and growth defects minimized. Using the data in Figs. 3 and 4, the normalized ratio of growth rate to defect concentration as a function of substrate temperature is plotted in Fig. 5. This ratio is a figure of merit for the efficiency of diamond growth, since large values of this ratio correspond to high growth rates and/or low defect densities. Between 800 and 1100 K, where growth rates increase with increasing temperature and defect concentrations are low, this ratio increases with increasing temperature. Above 1200 K, where defect concentrations become high, the ratio decreases with increasing temperature. Therefore, the results in Fig. 5 suggest that, for the growth environment simulated here, optimal growth temperatures are in the range of 1100 to 1200 K. This prediction is in accord with experimental observations[4] and previous kinetic calculations,[4,20] which indicate that ideal growth temperatures for hot-filament and microwave CVD growth of diamond are around 1200 K. However, we have not included

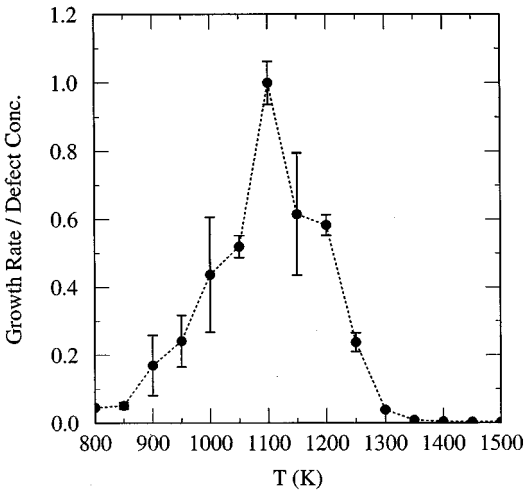

FIG. 5. Normalized efficiency of {111} diamond film growth, defined as the ratio of growth rate to defect concentration, as a function of substrate temperature in an environment containing 0.04, 18, 0.004, and 0.1 Torr partial pressure of H, H_2, CH_3, and C_2H_2, respectively. Error bars represent standard deviations over four simulations at each temperature.

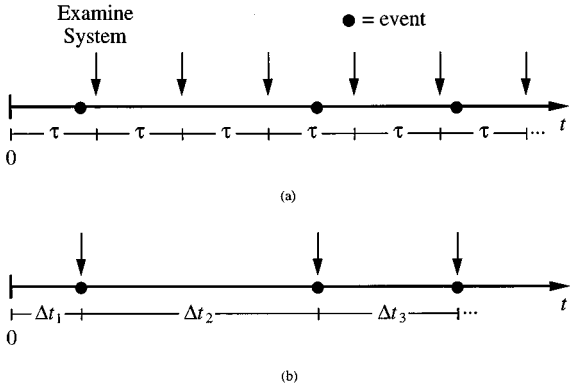

FIG. 6. Schematics of temporal sampling schemes in the (a) conventional kinetic Monte Carlo and (b) N-fold way Monte Carlo methods. In conventional schemes, the system is sampled at regular time intervals, τ, such that at most one event occurs in each interval. In the N-fold way scheme, the system is sampled only when an event occurs, and the time increment between events, Δt, is a variable.

the effects of twinning during growth,[1] and these results can only be applied to the growth of {111}-oriented single crystals. In addition, we have neglected the formation of sp^2-bonded C, which is often more important[4,20] to the quality of diamond films than vacancies or H atom defects. Nonetheless, the incorporation of sp^2-bonded C during single crystal growth should occur by the same overgrowth mechanism considered here,[4] and while these results cannot be directly used as quantitative predictions of {111} film quality *per se*, they are useful for estimating the effects of processing conditions on growth rates, growth defects, and growth efficiency.

SUMMARY

We have presented a kinetic Monte Carlo technique for simulating thin film growth by chemical vapor deposition on the atomic scale in three dimensions based on known reaction kinetics. The kinetics of the relevant surface processes and the effects of surface atomic structure and morphology are included in the model. Processes which involve cooperation between adjacent surface atoms, such as reconstruction and growth of {100} diamond facets, are handled explicitly on the atomic scale. The temporal evolution of the system is simulated using an N-fold way Monte Carlo scheme which employs a transition probability of one and a variable time increment, allowing the consideration of processes that occur on widely different time scales. The model is efficient enough to handle the growth of hundreds of atomic planes on substrates containing thousands of surface atoms, using only a desktop workstation. Because the model treats film growth on the atomic scale, it is useful not only for studying the evolution of film morphology and defect incorporation, but also as a tool for examining and verifying proposed atomic growth mechanisms.

The growth of {111}-oriented diamond films was simulated for several substrate temperatures ranging from 800 to 1500 K. Under typical CVD conditions, the growth rates vary from about 0.1 to 0.8 μm/hr between 800 and 1500 K, and the activation energy for growth on the {111} surface between 800 and 1100 K is 11.3 kcal/mol, in agreement with experiment and other simulations. The concentrations of incorporated point defects are low at substrate temperatures below 1300 K, but become high above this temperature. Therefore, in the growth environment simulated here, optimal {111} growth efficiency, defined as the ratio of growth rate to point defect concentration, can be achieved between approximately 1100 and 1200 K.

ACKNOWLEDGMENTS

The authors gratefully acknowledge the support of the Advanced Research Projects Agency and the Naval Research Laboratory under Contract No. N00014-96-1-G000. The authors also wish to thank J. E. Schnitker for enlightening discussions.

APPENDIX A: THE N-FOLD WAY TIME INCREMENT

Consider a system that evolves in time along a chain of configurations. In conventional kinetic Monte Carlo simulations,[30,39] a constant time increment is chosen such that *at most* one event occurs during each time increment. This is depicted schematically in Fig. 6(a). This approach is useful for studying the evolution of systems that can evolve through an infinite number of distinct events. However, if the number of events by which the system can evolve is finite and enumerable, then a more efficient approach can be adopted. Instead of examining the system at fixed time intervals, and calculating what events occur and when, the system can be examined only when an event occurs, and the time increment itself can be calculated at each step. This is depicted schematically in Fig. 6(b), and corresponds to the N-fold way approach.[28,29] Although this technique has clear advantages[28,29] in almost any Monte Carlo application wherein the number of possible events is finite, it is particularly useful in situations where the events occur on very different time scales[30] and the fastest events are only possible in

certain rare system configurations. Such is the case in these simulations of diamond CVD, where very fast events (e.g., dimer opening by reaction 11 and dimer insertion by reaction 12 in Table II) only occur under certain circumstances.

In the Monte Carlo scheme depicted in Fig. 6(b), the task is to determine (at each simulation step) the time increment that has elapsed since the last event. This can be accomplished as follows.[28] The probability that an event will occur during some infinitesimal time interval, dt, is simply Πdt, where Π is the probability that an event will occur in a unit time interval or, equivalently, the average number of events that occur per unit time. Therefore, the probability that *no* event occurs during time dt is $(1-\Pi dt)$. Let $t=0$ be the time at which the last (i.e., most recent) event occurred. Let the probability that *no* event occurs in time Δt (since the last event) be denoted $P(\Delta t)$. The probability that *no* event occurs during time $\Delta t+dt$, $P(\Delta t+dt)$, is equal to the probability that (1) no event occurs during Δt and (2) no event occurs during the following dt,

$$P(\Delta t+dt)=P(\Delta t)(1-\Pi dt). \tag{A1}$$

Equation (A1) can be rewritten as a differential equation,

$$\frac{dP}{dt}=-P(\Delta t)\Pi, \tag{A2}$$

which has the solution

$$P(\Delta t)=\exp(-\Pi\Delta t), \tag{A3}$$

since $P(0)=1$. In the Metropolis Monte Carlo algorithm,[39] configurational transitions which increase the system energy are either accepted or rejected based on a comparison between a Boltzmann distribution and a random number. Similarly, $P(\Delta t)$ is assigned a random number, ξ_2, evenly distributed in the range (0,1). Substituting for $P(\Delta t)$ and solving for Δt

$$\Delta t=-\frac{\ln(\xi_2)}{\Pi}, \tag{A4}$$

which can be compared directly to Eq. (2). This N-fold way approach is statistically equivalent to conventional Monte Carlo schemes.[29]

[1] R. C. DeVries, Annu. Rev. Mater. Sci. **17**, 161 (1987).
[2] K. E. Spear, J. Am. Ceram. Soc. **72**, 171 (1989).
[3] F. G. Celii and J. E. Butler, Annu. Rev. Phys. Chem. **42**, 643 (1991).
[4] J. E. Butler and R. L. Woodin, Philos. Trans. R. Soc. London, Ser. A **342**, 209 (1993).
[5] D. G. Goodwin and J. E. Butler, in *Handbook of Industrial Diamonds and Diamond Films*, edited by M. A. Prelas, G. Popovici, and L. K. Bigelow (Dekker, New York, 1997), pp. 527–582.
[6] F. G. Celii, P. E. Pehrsson, H.-t. Wang, and J. E. Butler, Appl. Phys. Lett. **54**, 2043 (1988).
[7] C.-H. Wu, M. A. Tamor, T. J. Potter, and E. W. Kaiser, J. Appl. Phys. **68**, 4825 (1990).
[8] W. L. Hsu, Appl. Phys. Lett. **59**, 1427 (1991).
[9] D. W. Brenner, Phys. Rev. B **42**, 9458 (1990).
[10] B. J. Garrison, E. J. Dawnkaski, D. Srivastava, and D. W. Brenner, Science **255**, 835 (1992).
[11] D. Huang and M. Frenklach, J. Phys. Chem. **96**, 1868 (1992).
[12] V. I. Gavrilenko, Phys. Rev. B **47**, 9556 (1993).
[13] Y. L. Yang and M. P. D'Evelyn, J. Am. Chem. Soc. **114**, 2796 (1992).
[14] T. Frauenheim, U. Stephan, P. Blaudeck, D. Porezag, H.-G. Busmann, W. Zimmermann-Edling, and S. Lauer, Phys. Rev. B **48**, 18189 (1993).
[15] Z. Jing and J. L. Whitten, Surf. Sci. **314**, 300 (1994).
[16] S. Skokov, C. S. Carmer, B. Weiner, and M. Frenklach, Phys. Rev. B **49**, 5662 (1994).
[17] S. Ciraci and I. P. Batra, Phys. Rev. B **15**, 3254 (1977).
[18] S. H. Yang, D. A. Drabold, and J. B. Adams, Phys. Rev. B **48**, 5261 (1993).
[19] B. N. Davidson and W. E. Pickett, Phys. Rev. B **49**, 11253 (1994).
[20] M. Frenklach and H. Wang, Phys. Rev. B **43**, 1520 (1991).
[21] S. J. Harris and D. G. Goodwin, J. Phys. Chem. **97**, 23 (1993).
[22] M. E. Coltrin and D. S. Dandy, J. Appl. Phys. **74**, 5803 (1993).
[23] D. S. Dandy and M. E. Coltrin, J. Mater. Res. **10**, 1993 (1995).
[24] M. O. Kaukonen and R. M. Nieminen, Surf. Sci. **331–3**, 975 (1995).
[25] E. J. Dawnkaski, D. Srivastava, and B. J. Garrison, J. Chem. Phys. **104**, 5997 (1996).
[26] M. M. Clark, L. M. Raff, and H. L. Scott, Comput. Phys. **10**, 584 (1996).
[27] C. C. Battaile, D. J. Srolovitz, and J. E. Butler, Diamond Relat. Mater. (in press).
[28] A. B. Bortz, M. H. Kalos, and J. L. Lebowitz, J. Comp. Physiol. **17**, 10 (1975).
[29] G. N. Hassold and E. A. Holm, Comput. Phys. **7**, 97 (1993).
[30] K. A. Fichthorn and W. H. Weinberg, J. Chem. Phys. **95**, 1090 (1991).
[31] R. Locher, C. Wild, N. Herres, D. Behr, and P. Koidl, Appl. Phys. Lett. **65**, 34 (1994).
[32] J. S. Kim and M. A. Cappelli, J. Mater. Res. **10**, 149 (1995).
[33] R. E. Rawles, W. G. Morris, and M. P. D'Evelyn, in *Diamond for Electronic Applications, Boston, MA*, edited by D. L. Dreifus, A. Collins, T. Humphreys, K. Das, and P. E. Pehrsson, Mater. Res. Soc. Symp. Proc. **416** (Materials Research Society, Pittsburgh, 1996), pp. 13–18.
[34] Y. L. Yang, L. M. Struck, L. F. Sutcu, and M. P. D'Evelyn, Thin Solid Films **225**, 203 (1993).
[35] B. D. Thoms, J. N. Russell, Jr., P. E. Pehrsson, and J. E. Butler, J. Chem. Phys. **100**, 8425 (1994).
[36] D. D. Koleske, S. M. Gates, B. D. Thoms, J. N. Russell, Jr., and J. E. Butler, J. Chem. Phys. **102**, 992 (1995).
[37] S. J. Harris and D. N. Belton, Jpn. J. Appl. Phys., Part I **30**, 2615 (1991).
[38] S. Skokov, B. Weiner, and M. Frenklach, J. Phys. Chem. **99**, 5616 (1995).
[39] N. Metropolis, A. W. Rosenbluth, M. N. Rosenbluth, A. H. Teller, and E. Teller, J. Chem. Phys. **21**, 1087 (1953).
[40] S. J. Harris, Appl. Phys. Lett. **56**, 2298 (1990).
[41] B. D. Thoms, M. S. Owens, J. E. Butler, and C. Sprio, Appl. Phys. Lett. **65**, 2957 (1994).
[42] B. D. Thoms and J. E. Butler, Surf. Sci. **328**, 291 (1995).
[43] S. J. Harris and A. M. Weiner, Appl. Phys. Lett. **53**, 1605 (1988).
[44] S. J. Harris and A. M. Weiner, J. Appl. Phys. **67**, 6520 (1990).
[45] F. G. Celii and J. E. Butler, J. Appl. Phys. **71**, 2877 (1992).
[46] D. S. Dandy and M. E. Coltrin, J. Appl. Phys. **76**, 3102 (1994).
[47] C. J. Chu, R. H. Hauge, J. L. Margrave, and M. P. D'Evelyn, Appl. Phys. Lett. **61**, 1393 (1992).
[48] C. Battaile, D. J. Srolovitz, and J. E. Butler, in *Thin Films: Surface and Morphology, Boston, MA*, edited by R. Cammarata, E. Chason, T. Einstein, and E. Williams, Mater. Res. Soc. Symp. Proc. **441** (Materials Research Society, Pittsburgh, 1997), pp. 509–514.